Fission in the region of radium and actinium

Yu. A. Selitskiĭ

V. G. Khlopin Radium Institute, Leningrad
Fiz. Elem. Chastits At. Yadra **10**, 314–355 (March–April 1979)

The experimental material on the fission of radium and actinium nuclei with its characteristic unusual triple-humped mass distribution of the fragments is systematized. For different excitation methods, the following data are presented: the fission cross sections and thresholds, the kinetic energies and angular distributions of the fragments, and the energy dependence of the symmetric and asymmetric fission components. Theoretical models that attempt to explain the triple-humped mass distribution of the fragments and its dependence on the excitation energy are discussed.

PACS numbers: 25.85.Ec, 25.85.Ge, 25.85.Jg, 27.90. + b

INTRODUCTION

After fission had been discovered, the main attention of physicists was directed toward the fission of uranium, thorium, and transuranium elements. In connection with the development of atomic energy, readily fissioning nuclei were of the greatest interest. However, despite numerous publications on such investigations, the main characteristic of fission—the mechanism governing the mass distribution of the fragments—has not been elucidated. Whereas nuclei with $Z = 90$–98 most probably undergo asymmetric fission at low and medium excitations, nuclei lighter than astatine are characterized by a "liquid-drop" symmetric mass distribution of the fragments in the case of above-barrier excitations ~10 MeV. One might expect radium and actinium, which lie between these two groups, to exhibit a preference for asymmetric fission, but with a smaller dip between the humps than for heavy nuclei. Jensen and Fairhall's experiment in 1958 on fission of radium induced by protons gave a remarkable result, a triple-humped mass yield curve for the fragments being obtained (Fig. 1).[1] This complicated form appeared to be a superposition of double-humped asymmetric fission and single-humped symmetric fission. Similar results were obtained in the case of excitation of radium by deuterons,[2] α particles,[2] γ rays,[3] and neutrons[4] of medium energies. The properties of these nuclei are unusual in not only the triple-humped mass yield curves. Experiments showed that for nuclei lighter than thorium, the approximate constancy of the height of the fission barrier characteristic for nuclei with $Z \geqslant 90$ is replaced by a rapid increase of the height; other distinctive features are the transformation of the mass yield curve with increasing excitation energy, the angular distributions of the fragments, and the dependence of the number of evaporated neutrons on the fragment mass. Thus, the fission of radium and actinium does not represent an ordinary particular case in a fairly long list of fissile nuclei but is the most complicated phenomenon in fission.

During the four decades that have elapsed since the discovery of fission, there have been developed a number of theoretical models which describe the main properties of the reaction with varying degrees of completeness. Each of the models requires experimental verification. In this respect too, by virtue of their complexity, the experimental fission characteristics of intermediate nuclei such as Ra and Ac present the toughest test for the correctness and universality of these models.

In the present review, we systematize the experimental material bearing on the fission of Ra and Ac and consider the existing theoretical explanations of it in the framework of various models. Hitherto, this question has been treated only in original papers, or individual characteristics of the fission have been analyzed without an adequate coverage of the bibliography.

1. FISSION CROSS SECTIONS AND BARRIERS OF THE RADIUM AND ACTINIUM ISOTOPES

Fission Cross Sections. The study of nuclei in the region between bismuth and thorium is complicated by their high specific activity and comparatively small fission cross sections. In practice, it is possible to prepare targets only with the longest-lived ^{226}Ra ($\tau_{1/2} = 1622$ years) and ^{227}Ac ($\tau_{1/2} = 22$ years). Let us first consider the known fission cross sections of these nuclei, and then analyze the threshold energies or barrier heights obtained from them. In the first stage of experimental investigation, Ra was bombarded mainly with charged particles,[1,2,5–9] since the large fluxes of charged particles made it possible to compensate for the low fissility of radium. The cross sections of fission by charged particles have a steep energy dependence (Fig. 2) due to the influence of the Coulomb interaction. The Coulomb barrier is

$$B_{\text{Coul}} = Z_1 Z_2 e^2/[r_0 (A_1^{1/3} + A_2^{1/3})],$$

where the subscripts 1 and 2 refer to the target nucleus and the incident particle. For the considered nuclei and singly charged particles, $B_{\text{Coul}} \approx 14$ MeV. As will be seen from the following determinations, the Coulomb barrier of radium and actinium is much higher than the fission barrier ($B_{\text{Coul}} - B_f \approx 7$ MeV), and this has the consequence that the fission cross section decreases rapidly with decreasing excitation of the compound nuclei long before B_f is approached. Thus, the direct determination of B_f from the rapid falloff of the fissility when radium is bombarded by charged particles proved impossible. The calculation of B_f using models was too uncertain, and therefore the Coulomb barriers of the intermediate nuclei remained unknown. Complications of this kind are not present in the case of neutrons or γ rays as incident particles.

 0090-4759/79/020121-18$02.80

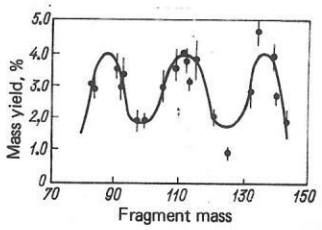

FIG. 1. Distribution of fragment masses from fission of ^{226}Ra by 11-MeV protons.[1]

The cross sections of the reactions ^{226}Ra(n,f) (Refs. 11–14) and ^{227}Ac(n,f) (Ref. 15) were measured by means of mica track detectors,[16] which have a high fragment detection efficiency and are virtually insensitive to particles with $Z \leq 20$, i.e., to the intense α emission of the targets. The $\sigma_{n,f}$ curves (^{226}Ra and ^{227}Ac) in Fig. 3 correspond to the lightest nuclei for which neutron fission cross sections have been measured. Comparison of them with similar measurements for heavier nuclei shows that perfectly natural changes take place with decreasing Z: 1) the threshold energy of the neutrons increases, 2) there is a rapid decrease in $\sigma_{n,f}$, 3) whereas the ^{227}Ac excitation function still exhibits the step profile associated with the thresholds of the $(n,n'f)$ and $(n,2n'f)$ reactions, in Ra it has virtually disappeared because of the steep energy dependence of the width ratio $\Gamma_f/\Gamma_{n'}$.

The difficulties of working with radium and actinium targets led to appreciable discrepancies between the cross sections measured in different experiments. For example, in Ref. 4, in contrast to Refs. 11–14, a fission threshold in the reaction ^{226}Ra(n,f) was not found, probably because of admixture in the target of heavier elements. Despite the large value of $B_f(^{227}\text{Ra})$, a paper has been published[18] with a remarkably large cross section for fission of ^{226}Ra by thermal neutrons. This result was not confirmed in Refs. 19 and 20, which gave the upper limit $\sigma_f(^{226}\text{Ra}+n_{\text{thermal}}) \leq 0.03$ mb for the cross section. As was shown in Ref. 15, the cross section for fission of ^{227}Ac by reactor neutrons determined in Ref. 21 is unreasonably large, and the overestimation can be attributed to the fission of daughter elements accumulating from the decay of ^{227}Ac.

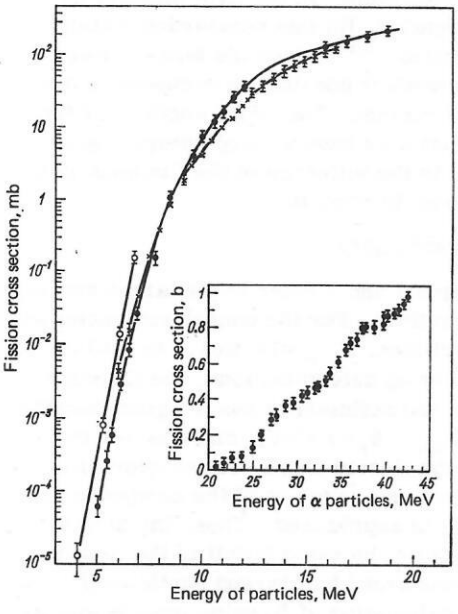

FIG. 2. Cross sections of ^{226}Ra and ^{227}Ac fission by charged particles. The crosses correspond to ^{226}Ra$+p$ (Refs. 6 and 7); the black circles to ^{226}Ra$+d$ (Refs. 7 and 9); the open circles to ^{227}Ac$+d$ (Ref. 10); in the insert, ^{226}Ra$+\alpha$ (Ref. 5).

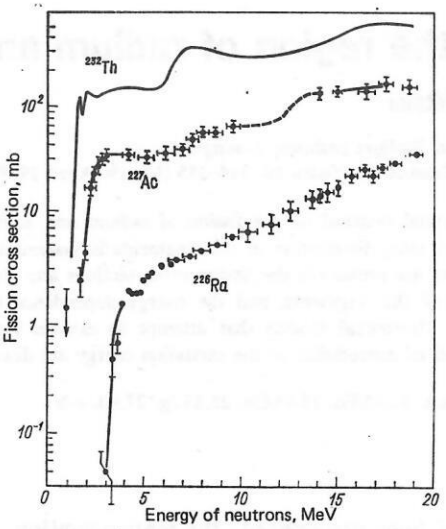

FIG. 3. Cross sections of fission by neutrons of the target nuclei ^{226}Ra (Refs. 11–14), ^{227}Ac (Ref. 15), and ^{232}Th (Ref. 17).

In addition to the neutron experiments, photofission experiments have been made to obtain information about the Ra and Ac barriers; these used bremsstrahlung γ rays from powerful linear electron accelerators and microtrons. In experiments using a bremsstrahlung spectrum of γ rays with limiting energy E_0, the fissility is characterized by the fission yield $Y(E_0)$, which is the number of fission events in the target per nucleus and per unit flux of γ rays. The photofission yield is a function that depends on the cross section of fission by monoenergetic γ rays, $\sigma_{\gamma,f}(E_\gamma)$, and the profile $W(E_\gamma, E_0)$ of the bremsstrahlung spectrum:

$$Y(E_0) = \alpha \int_0^{E_0} \sigma_{\gamma,f}(E_\gamma)\, W(E_\gamma, E_0)\, dE_\gamma,$$

where α is a coefficient of proportionality determined by the normalization of the bremsstrahlung spectrum.

In the first experiment of this kind,[3] it was found that the photofission yield of Ra at $E_0 = 23$ MeV is about 100 times smaller than for ^{238}U. Subsequently, measurements were made of the photofission yield curves for ^{226}Ra (Refs. 22 and 23) and ^{227}Ac, from which the cross sections $\sigma_{\gamma,f}$ were obtained by solving the above integral equation. The energy dependence of the photofission cross section has the giant resonance profile typical of dipole absorption of γ rays (Fig. 4). The curve of the energy dependence of the ^{227}Ac photofission cross section is split into two resonances corresponding to dipole vibrations along the elongation axis of the nucleus (the left-hand peak in Fig. 4) and vibrations in the perpendicular direction. This second collective motion has a doubled statistical weight,[24] and the area under the right-hand resonance in Fig. 4 is accordingly greater. The splitting of the giant resonance, which is a conse-

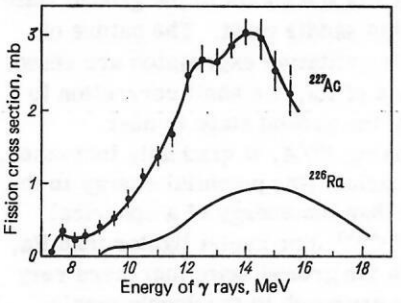

FIG. 4. Photofission cross sections of ^{226}Ra (Ref. 23) and ^{227}Ac.

quence of the deformation of the nucleus in the ground state in the form of an ellipsoid of revolution, makes it possible to calculate the ratio a/b of its axes.[24] For ^{227}Ac, it is found that $a/b = 1.15$, which is close to the value obtained from spectroscopic experiments.[26] The calculation of $\sigma_{\gamma,f}(^{226}\text{Ra})$ in Ref. 23 follows the common practice of using not the experimental $Y(E_0)$ values, but the averaged values of the photofission yield curve. For this reason, the photofission excitation function of radium in Fig. 4 is given without plotting of the calculated, and accordingly averaged, values of $\sigma_{\gamma,f}$. The energy interval between the experimental points in the photofission yield curve of Ra was 1 MeV, i.e., it was too large to reveal the double-humped profile of the excitation function. But the half-widths of the giant resonances of Ra and Ac are approximately the same, i.e., close to their deformation in the ground state. Both these nuclei occupy an intermediate position between the spherical Pb with closed N and Z shells and the strongly deformed heavier nuclei such as thorium and uranium with $a/b \approx 1.25$ (Ref. 25).

Data on the Ra and Ac fission cross sections for different types of excitation are given in Table I.

Fission Barriers. It was noted above that, as in the case of fission of even-even target nuclei with $Z \geq 90$ by neutrons, the dependences of the ^{226}Ra and ^{227}Ac fission cross sections on the neutron energy exhibit a threshold. In such cases, B_f is determined on the basis of the formula for the penetrability of a parabolic barrier obtained by Hill and Wheeler[28]:

$$P_f = \left[1 + \exp\left(\frac{B_f - E^*}{\hbar\omega/2\pi}\right)\right]^{-1}, \qquad (1)$$

where E^* is the excitation energy of the compound nucleus and $\hbar\omega$ is the curvature parameter of the barrier.

TABLE I. Fission cross sections of Ra and Ac.

Reaction	Energy of particles, MeV	Fission cross sections, cm^2	References
^{226}Ra+p	6—16.5	$4\cdot10^{-30}$—10^{-25}	[2, 5, 6, 7]
^{226}Ra+p	11—100	arbitrary units	[8]
^{226}Ra+d	5—21	$6\cdot10^{-32}$—$2\cdot10^{-25}$	[2, 5, 7, 9]
^{227}Ac+d	4—7	$1.3\cdot10^{-32}$—$1.5\cdot10^{-28}$	[10]
^{226}Ra+α	21—43	$2\cdot10^{-26}$—10^{-24}	[5]
^{226}Ra+n	3—19	$4\cdot10^{-29}$—$3.3\cdot10^{-26}$	[4,11—14]
^{223}Ra+n_{reactor}	—	$\sim 7\cdot10^{-25}$	[26]
^{226}Ra+n_{thermal}	—	$\leqslant 7\cdot10^{-30}$	[19, 20]
^{227}Ac+n	0.9—18.6	$1.3\cdot10^{-27}$—1.4^{-25}	[15]
^{227}Ac+n_{thermal}	—	$\leqslant 3\cdot10^{-28}$	[27]
^{226}Ra+γ	$\leqslant 20$	$\leqslant 10^{-27}$	[22, 23]
^{227}Ac+γ	$\leqslant 15.5$	$\leqslant 3\cdot10^{-27}$	

At low excitations, σ_f in a certain approximation is directly proportional to the fission width Γ_f or the extent to which the lowest channel is open:

$$\sigma_f \sim \Gamma_f \sim P_f.$$

In this case, the fission barrier is numerically equal to the excitation E^*_{thr} at which σ_f is half the cross section in the region of transition to the plateau:

$$B_f(A+1) = E^*_{\text{thr}} = E_{n\ \text{thr}} + B_n(A+1), \qquad (2)$$

where A is the mass number of the target nucleus, and $B_n(A+1)$ is the binding energy of a neutron in the compound nucleus.

The determination of B_f in this method is approximate for the following reasons:

1) No allowance is made for the contribution to Γ_f of the channels lying above the lowest state. 2) No allowance is made for the complicated shape of the barrier. As was shown by Strutinskiĭ[29,30] and other investigators, shell structure is preserved in nuclei despite deformation. In the general case, this leads to a complicated shape of the barrier and the appearance of resonances in the subthreshold region of σ_f due to levels in the second potential well. 3) In the region of the threshold, the widths Γ_n and Γ_γ and the neutron capture cross section σ_c are taken to be approximately constant.

However, a comparison of B_f calculated by means of (2) and examples of a more rigorous channel analysis[31] shows that the difference between the calculated B_f does not exceed 0.2–0.3 MeV; this is so because of the steep falloff of σ_f in the threshold region. For this reason, the above simplified approach is frequently used in the absence of detailed information about the channel structure of the states at the saddle point.

The fission barriers of the Ra and Ac isotopes determined from the thresholds of the (n,f), $(n,n'f)$, and $(n,2n'f)$ reactions in the neutron excitation functions, from the steep falloff in the photofission yield curves, and from the calculated photofission cross sections are given in Table II. The cross section of fission of radium by neutrons increases monotonically with increasing E_n without the steps observed in the case of heavier nuclei (see Fig. 3), and therefore the thresholds in its emission fission were identified by the changes in the angular distributions of the fragments (Sec. 4).

A number of papers have been published in recent

TABLE II. Comparison of experimental and theoretical heights of the fission barriers of radium and actinium (in MeV).

Nucleus	$B_{f,\text{exp}}$	$B_{f,\text{theor}}$ with allowance for shell corrections and asymmetry	B_f, ldm (Ref. 32)
^{228}Ra	8.2—8.9 [33]	8.2 [34]; 8.7 [35]	7.4
^{227}Ra	8.3±0.3 [11—14]		7.2
^{226}Ra	8.5±0.5 [11, 22, 23]	8.5 [36]; 9.0 [35]	7.0
^{225}Ra	7.6±0.5 [37]	—	6.5
^{228}Ac	7.2±0.2 [15, 38, 39]	—	5.7
^{227}Ac	7.0±0.5 [15]	—	5.5
	7.3 [38, 39]	—	—
	7.6±0.3 from (γ, f) reaction; (see Fig. 4)	—	—

years in which the fissility ($W_f = \Gamma_f/\Gamma$) of the Ra and Ac isotopes is deduced from direct reactions.[33,38,39] For example, the fissility for bombardment by deuterons is defined as

$$W_f = \sigma(d, pf)/\sigma(d, p).$$

The barrier heights of ^{227}Ac and ^{228}Ac were estimated in Refs. 38 and 39 at 7.3 and 7.2 MeV, respectively, in agreement to within the errors with the results of the experiment of direct bombardment of ^{227}Ac by neutrons in Ref. 15.

In Fig. 5, the complete set of values obtained for B_f (Ra, Ac) is shown as a function of the fissility parameter Z^2/A. For such comparisons, one frequently uses a parameter that is convenient in theoretical calculations:

$$x = E_{\text{Coul}}/2E_{\text{surf}} \sim Z^2/A,$$

where E_{Coul} is the energy of the Coulomb interaaction of protons of a spherical nucleus, and E_{surf} is its surface energy. To eliminate the ambiguity in x for a given nucleus due to the fact that different authors use different coefficients of proportionality in the expressions for E_{Coul} and E_{surf}, the abscissa in Fig. 5 is the value of Z^2/A, which is unique for a given nucleus. The experimental barriers of nuclei outside the region of the Ra and Ac isotopes are taken from the review of Ref. 40, and B_f(^{216}Rn) is taken from Ref. 41. As can be seen in Fig. 5, B_f begins to increase in nuclei lighter than thorium, and in the region of Rn and Ac it has the steepest growth. In contrast to this irregular dependence, the liquid-drop fission barrier varies smoothly.[32] In calculations of different authors, the absolute value of $B_{f,\text{ldm}}$ is different, depending, for example, on the parametrization, the allowance made for the diffuseness of the boundary of the nucleus, and the coefficient of surface tension; however, the relative change in $B_f = f(Z^2/A)$ is always monotonic and proportional to $(1-x)^3$. To illustrate these differences in the calculation of $B_{f,\text{ldm}}$, two curves, from Refs. 32 and 42, are shown in Fig. 5. One can choose the constants in the calculation of $B_{f,\text{ldm}}$ in such a way as to obtain agreement with $B_{f,\text{exp}}$ in some narrow region of Z^2/A, but this leads to a pronounced discrepancy with the $B_{f,\text{exp}}$ of the other nuclei.

The discrepancy between $B_{f,\text{exp}}$ and $B_{f,\text{ldm}}$ can be explained by the influence of the shells in the ground state of the nucleus and at the saddle point. The nature of this influence and its quantitative expression are shown in Fig. 6. In the region of Ra, the shell correction to the potential energy of the ground state is near zero.[34,43] With increasing Z^2/A, it gradually increases, reaching 2.5 MeV at curium (the potential energy in the ground state is lower than the energy of a spherical liquid-drop nucleus).[34,40,43] For nuclei lighter than Ra, the shell correction in the ground state increases very rapidly because of the approach to the doubly magic nucleus with $Z = 82$ and $N = 126$ and reaches ~14 MeV.[42,44] This effect also explains the rapid rise of $B_{f,\text{exp}}$ in the nuclei ^{216}Rn–^{209}Bi. The shell correction at the large deformations of the actinide nuclei is manifested in the formation of a second deep potential well (shape isomerism). In contrast, the correction $B_{f,\text{ldm}}$ is around 0–3 MeV and in nuclei lighter and heavier than plutonium is associated with the outer and inner barrier, respectively (see Fig. 6).[34,42,43] The upshot is that in the actinides heavier than Th the shell corrections in the ground state and at the saddle point lead to the approximate constancy $B_f \approx 6$ MeV (see Fig. 5).

Calculations for the even-even nuclei ^{226}Ra and ^{228}Ra adjacent to the actinides with allowance for the asymmetry at the saddle point indicate that B_f increases to 8–9 MeV.[34,42,32,35] The best agreement with the experiments was achieved in Refs. 34 and 36 (see Table II). According to these calculations, the deformation potential energy of the radium nuclei has the following characteristic features:

1) The fission barrier is always double-humped, and the outer barrier B_{f2} is the higher (the absence of isomeric fission of Ra and Ac (Ref. 45) also supports this conclusion).

2) The difference between the barrier heights B_{f2} and B_{f1} for the different Ra isotopes is approximately the same and about 5–6 MeV.

3) The outer barrier B_{f2} has its least height in the case of asymmetric deformation with asymmetry pa-

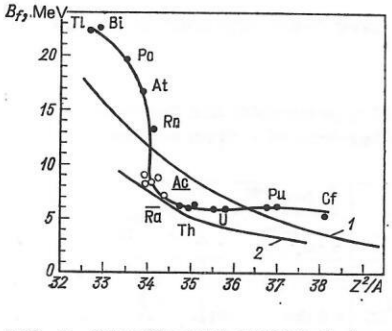

FIG. 5. Experimental and liquid-drop fission barriers. The open circles are B_f (Ra and Ac) on the basis of the data of Refs. 11–15, 23, 33, 37–39; the black circles are B_f from Ref. 40; B_f (^{216}Rn) is from Ref. 41; 1) $B_{f,\text{ldm}}$ (Ref. 42); 2) $B_{f,\text{ldm}}$ (Ref. 32).

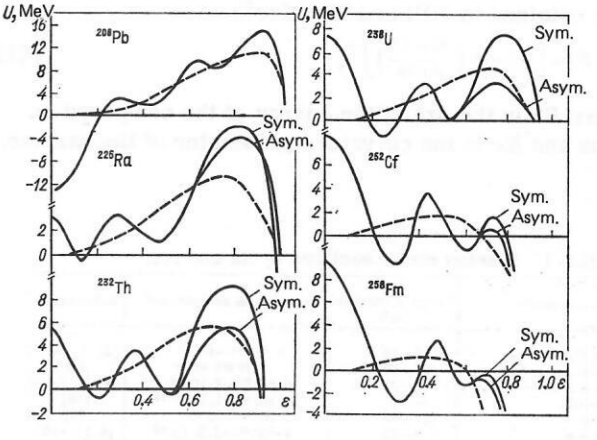

FIG. 6. Deformation potential energies corresponding to fission through the symmetric and asymmetric saddle points. The dashed curve is the liquid-drop barrier for symmetric fission.[43]

rameter corresponding to mass ratio 1.2–1.6 of the fragments that are formed.[35,43] The outer barrier for symmetric deformation of the nucleus is 1–2 MeV higher.

In later, more accurate calculations, Möller and Nix[44] found a splitting in the light actinides of the barrier B_{f2} into two humps of approximately equal height with a small dip ~1 MeV between them. This makes it possible to explain the experimentally observed resonances in the near-threshold fissility of ^{233}Th and ^{231}Th.[31] It was suggested in Refs. 35 and 39 that the second hump of ^{228}Ra and ^{227}Ac could be split in this manner. The shell corrections to the potential energy and the fission barriers of the odd nuclei of Ra and Ac have not yet been calculated. As can be seen from Table II, the experimental B_f do not exhibit even-odd differences to within the errors. The same property of B_f was noted in heavier nuclei in Refs. 40 and 47.

Thus, measurements of the heights of the fission barriers of ^{216}Rn and of the isotopes of Ra and Ac have filled the existing gap between W and Th. The dependence of B_f on Z^2/A of fissile nuclei can be best explained with allowance for their shell structure at all stages of deformation from the ground state to the saddle point.

2. ASYMMETRY OF THE FRAGMENT MASS DISTRIBUTION

The triple-humped mass distribution of the fragments of the Ra and Ac nuclei at medium excitation energies is their characteristic and most remarkable property. With the accumulation of experimental data and the development of fission theory, different suggestions have been made as to the nature of this complicated mass distribution; we shall discuss these below.

Superposition of Emissionless and Emission Fission. Properties of the Mass Yield Curve up to the Threshold of Emission Fission. Figure 1 shows the first triple-humped mass yield curve of the fragments obtained radiochemically in 1958 by Jensen and Fairhall for fission of ^{226}Ra by 11-MeV protons.[1] Jensen and Fairhall assumed that the three humps are due to simple superposition of strongly excited symmetric[1)] fission of the compound nucleus ^{227}Ac and the asymmetric distribution of the fission fragments of ^{226}Ac nuclei cooled first by the evaporation of neutrons. Although other suggestions were made, the paper of Perry and Fairhall[7] in 1971 on Ra fission by deuterons and protons seemed to confirm the first suggestion. In this experiment, the mass distribution of post-emission fission measured in the reaction $^{226}\mathrm{Ra}+p\rightarrow{}^{227}\mathrm{Ac}-f$ was subtracted from the fragment distribution of ^{228}Ac excited to $E^*=24$ MeV. It was found that the difference curve of pure pre-emission fission of ^{228}Ac has a symmetric single-humped distribution. However, the experiment was flawed by the too high excitation of the initial compound nuclei. It is known that the yield of fragments at the symmetric peak increases rapidly with increasing excitation. Therefore, asymmetric fission unrelated to cooling of the nuclei by neutron emission could have had an effect not noted in Ref. 7 on the background of the predominant symmetric peak. Perry and Fairhall noted the need for measurement at low excitations, in which emission fission could not exist on energy grounds. It is precisely in this region that one would like to know if the mass distribution of the fragments retains the three humps.

A critical experiment of this kind was performed at the present author's institute[13,14] on ^{226}Ra using neutrons with energy $E_n=5$–15 MeV (the threshold of emission fission is in the region of $E_n=9$ MeV). The absence of the Coulomb barrier made measurements at low E^* possible. Information about the mass yield curve could be extracted from the spectra of the kinetic energy E of the fragments without pair coincidences. Because of the specific nature of Ra fission, this was sufficient to estimate the fraction of the total number of fission events at the central peak of the mass yield curve. With a measurement of the energy of only one of the pair of fragments, it was possible to place the radium target almost immediately next to the neutron source in a region of particle flux of high specific density, i.e., one could significantly increase the rate of collection of information compared with an experiment in which the energies of two equal fragments are measured separately. Figure 7, in which the kinetic energy spectra of the Ra fission fragments in the laboratory coordinate system are plotted, shows that the symmetric fission peak is predominant at $E_n=15$ MeV. With decreasing neutron energy, the contribution of symmetric fission rapidly decreases, and at $E_n=5$ MeV the spectrum has a profile similar to the spectra of heavy asymmetrically fissioning nuclei. One can also see that in all the spectra of Fig. 7 a well-defined minimum separates the peak of light fragments of asymmetric fission from the total distribution of the heavy fragments and the fragments of symmetric fission. This feature of the spectra reflects, first, the circumstance that the mean total kinetic energy of symmetric fission is lower than that of asymmetric fission and, second, the fact that the difference between the most probable energies of the light and the heavy fragment is large in the case of Ra fission (among all the asymmetrically fissioning nuclei, Ra, as the lightest nucleus, has the most asymmetric most probable mass distribution). This property of the spectra made it possible to separate in them the group of light fragments by extrapolating the slopes of the curves to the right and left of the minima to the abscissa (the dashed curves in Fig. 7). If we denote the number of light fragments in the right-hand peak of the curves by N_1, then the remaining part N_2 includes the heavy fragments of asymmetric fission and the symmetric-fission peak. In this case, the fractions of

---

[1)]Here and in what follows, we understand by "symmetric" fission the relative total yield of fragments in the region of the peak with the most probable fragment masses $m_1=m_2$. "Asymmetric" fission is defined similarly. It can be shown that the calculation of the relative yield of the components does not depend on whether the peaks are approximated by Gaussian curves[6,44] or by a splitting into three sections whose boundaries are determined by the minima in the mass yield curve.[38,39]

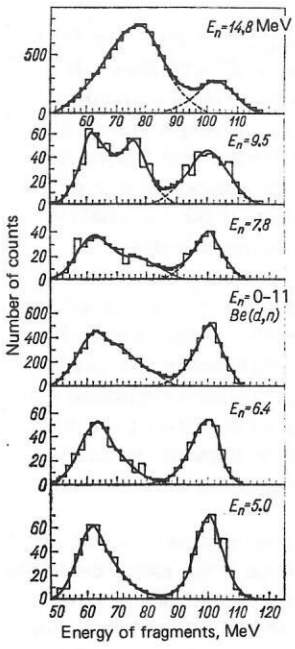

FIG. 7. Kinetic energy spectra of fragments in the laboratory coordinate system for ^{226}Ra fission by neutrons of different energies.[13,14] The d spectrum is at effective neutron energy ~7.6 MeV; the neutrons were obtained by bombarding a thick beryllium target with 6.8-MeV deuterons.

symmetric and asymmetric fission, s and a, are

$$s=\frac{N_2-N_1}{N_1+N_2}; \quad a=1-s. \tag{3}$$

The results of calculations in the form of the dependence $s(E_n)$ are shown in Fig. 8a. Besides the energy scale of the neutrons, this gives the scale of the excitation energy of the fissioning nucleus E^*. Figure 8b shows the separation of the total cross section σ_f of Ra fission by neutrons into the symmetric, $\sigma_{fs}=s\sigma_f$, and asymmetric, $\sigma_{fa}=a\sigma_f$, fission. It is interesting that the component σ_{fa} in the region $E_n \leq 9$ MeV has the plateau section characteristic of heavy, asymmetrically fissioning nuclei, and that the dependence $\sigma_{fs}(E^*)$ is reminiscent of the cross section profile of light fissile nuclei.

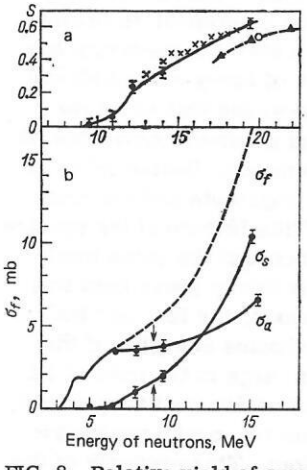

FIG. 8. Relative yield of symmetric fission as a function of the neutron energy or the excitation energy of the compound nuclei (a). The symmetric (σ_s) and asymmetric (σ_a)) components of the cross section of Ra fission by neutrons (b). The black circles correspond to ^{226}Ra+n (Refs. 13 and 14); the crosses to Ra+p (Ref. 6); the black triangles to ^{226}Ra+d (Ref. 48); the open circles to ^{226}Ra+d (Ref. 49); the dashed curve is the total fission cross section σ_f; the arrow indicates the threshold of the ^{226}Ra(n,n',f) reaction.

As a result, it was possible to draw the following conclusions: 1) In the region of energies near the fission barrier, Ra undergoes asymmetric fission, like heavier nuclei. 2) At higher energies, up to $E^* \leq 13.5$ MeV, where there is still no emission fission, fission of the compound nucleus ^{227}Ra is characterized by a triple-humped mass yield curve of the fragments. Before the threshold of the ^{226}Ra($n,n'f$) reaction, 30% of the total number of fission events already corresponds to the fraction of the symmetric peak. 3) With increasing excitation, the mass yield of the symmetric component grows faster than that of the asymmetric component. Symmetric fission becomes significant when E_n exceeds a threshold value at about 2 MeV; increasing rapidly, it becomes predominant.

Thus, on the basis of the conclusion 2 (see Fig. 8), it became obvious that Jensen and Fairhall's explanation[1] of the triple-humped mass yield curve as a superposition of emission and emissionless fission is untenable.

Six months after the neutron experiments described above, similar results and conclusions were obtained by Konecny *et al.*[38] for the nuclei ^{227}Ac and ^{228}Ac formed at low excitations by a direct stripping reaction before the fission event (Fig. 9). This very convenient method made it possible to carry out more accurate and detailed measurements and, using different stripping and capture reactions, to obtain in subsequent experiments[33,39] information about the symmetric and asymmetric fission of ^{225}Ra, ^{227}Ra, ^{228}Ra, and ^{226}Ac. The traditional separation of symmetric fission on the basis of the energy of a pair of equal fragments made it possible to follow the decrease right down to ~10^{-2} of the

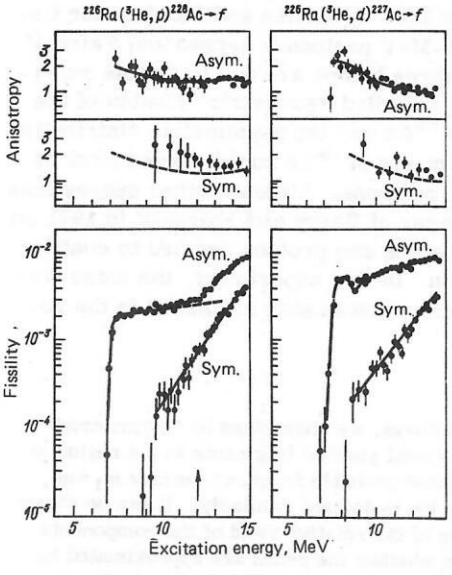

FIG. 9. Fission probabilities and anisotropy of the symmetric and asymmetric components of ^{227,228}Ac fission.[38]

asymmetric yield. The energy dependence of P_s/P_a or Γ_{fs}/Γ_{fa} exhibits an inflection at an excitation energy 1.0–2 MeV above the barrier of asymmetric fission. Although the accuracy of the measurements in this region is poor, it is concluded in Refs. 33, 38, and 39 that there is a difference between the barriers B_{fs} and B_{fa} ($B_{fs} - B_{fa} = 1$–2 MeV). It is noted in Ref. 49 that the dependence of Γ_{fs}/Γ_{fa} on the excitation energy above the barrier has the same steepness for all nuclei (Fig. 10). However, in my opinion this cannot be completely correct, since only nuclei for which symmetric fission is represented simply by a dip between the asymmetric humps have the same steepness in $\Gamma_{fs}/\Gamma_{fa} = f(E^* - B_f)$. And the nuclei Ra and Ac, which have a well-defined triple-humped distribution, exhibit strongly differing Γ_{fs}/Γ_{fa} slopes in Fig. 10.

All the features regarding the relative yield of symmetric fission noted above are also manifested in the investigation made in Refs. 51 and 52 of the ^{226}Ra(γ, f) reaction, i.e., the properties are observed to be independent of the parity of the number of nucleons in the compound nucleus and the method of its formation (Fig. 11).

The Hypothesis of Two Types of Fission. This was long regarded as an alternative explanation for the triple-humped mass distribution of the fragments. It was proposed in 1951 by Turkevich and Niday[53] on the basis of observation of a small peak of symmetric fission between two predominant humps of ordinary asymmetric fragment mass yield in the case of bombardment of ^{232}Th with reactor neutrons. Without establishing more precisely the physical nature of the phenomenon, Turkevich and Niday suggested that the mass yield curve of the fragments in the general case is a superposition of two distribution curves with a single hump (symmetric) and with two humps. It should be noted that this hypothesis has nothing in common with the superposition of emission and emissionless fission, because, for a start, the fission of ^{232}Th by neutrons is characterized in both cases by a predominantly asymmetric mass distribution of the fragments. The suggestion that the reaction could develop through two independent channels had fundamental significance and

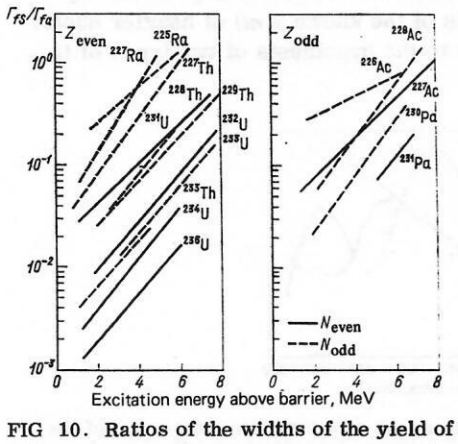

FIG 10. Ratios of the widths of the yield of the symmetric and asymmetric fission components as a function of the excitation energy above the barrier.[50]

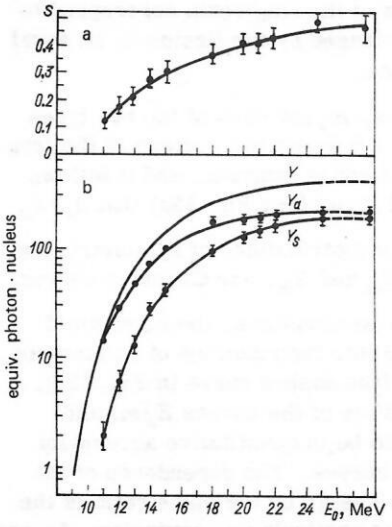

FIG. 11. Relative yield of the symmetric fission component (a) as a function of the limiting energy of the γ- ray bremsstrahlung spectrum and decomposition of the total photofission yield Y into the yields of the components of symmetric, Y_s, and asymmetric, Y_a, fission.[52]

stimulated numerous studies, including both qualitative experimental investigations and others with a quantitative analysis[54,55] of the hypothesis.

Because of the clearly expressed three humps, fission of Ra–Ac nuclei is the most convenient phenomenon for testing the hypothesis. One of the most complete experiments was made by Britt *et al.*,[48] who bombarded ^{226}Ra with protons, deuterons, and α particles of different energies. In contrast to Ref. 1, they assumed that admixture of emission fission of Ra does not have an appreciable significance. Measuring the kinetic energy of pair fragments corresponding to the same fission event, they obtained the fragment mass yield curves $W(m)$, the dependence of the total kinetic energy of the two fragments on their mass ratio $E_k(m)$, and the variance $\sigma^2[E_k(m)]$ for different mass ratios. As an example, Fig. 12 shows the results of bombardment of ^{226}Ra with 14-MeV deuterons. All these characteristics were analyzed quantitatively from the point of view of the superposition of two types of fission. The analysis was based on a number of assumptions:

1) The kinetic energy of the fragments is equal to their Coulomb energy at the scission point.

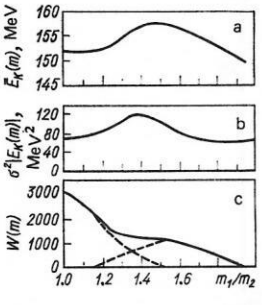

FIG. 12. Mean kinetic energy (a), variance of the distribution $E_k(m)$ (b), and fragment mass yield (c) as functions of the ratio of the fragment masses in ^{226}Ra fission by 14-MeV deuterons.[48]

2) The mean charges of the fragments correspond to the maximal energy released by the fission or an equal length of β-decay chains.

3) For all values of m_1/m_2 for each of the two types of fission the distance d between the centers of the fragments at the scission point is constant, and it follows from the experimental $E_k(m)$ (see Fig. 12a) that $d_s > d_a$.

4) The kinetic-energy distributions of symmetric and asymmetric fission, E_{ks} and E_{ka}, are Gaussian curves.

On the basis of these assumptions, the mass yield curve was decomposed into distributions of symmetric and asymmetric form (the dashed curve in Fig. 12b), and the calculated profiles of the curves $E_k(m)$ and $\sigma^2[E_k(m)]$ were found to be in quantitative agreement with the experimental curves. The dependence of the variance of the kinetic energy on the mass ratio of the fragments seemed to be particularly convincing. As can be seen in Fig. 12b, $\sigma^2[E_k(m)]$ has maximal value in the region of overlap of the hypothetical independent distributions. This result was regarded as a natural consequence of the difference between the most probable E_k for the two distributions at the same ratio m_1/m_2.

It seemed that even more definite evidence for the superposition of two independent distributions could be obtained by measuring not the variance, but the profile of the E_k distribution for different m_1/m_2. This was the reason for the writing of Ref. 49, in which it was expected that a distribution of a symmetric type of fission could be separated from the asymmetric distribution through its inherent greater deformation of the fragments or lower kinetic energy. By means of the measurement of the energy of equal fragments, a contour diagram was obtained for the fission of ^{226}Ra by 12-MeV deuterons (Fig. 13), and the profile of the E_k distributions for different m_1/m_2 was obtained (Fig. 14). Unfortunately, an ambiguous result was obtained: the separation of the E_k distributions into two peaks did not occur, although the change in the asymmetry of the profile of the curves corresponded exactly to what one would expect from the superposition of two independent

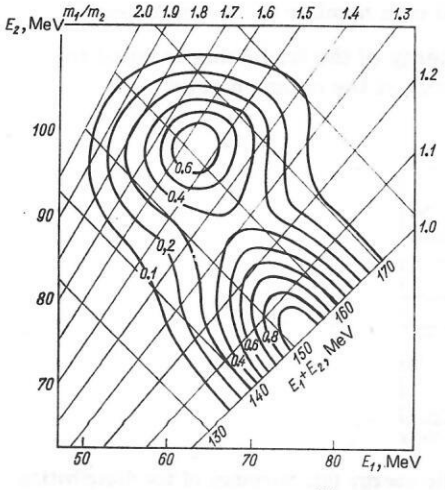

FIG. 13. Contour diagram of ^{226}Ra fission by 12.1-MeV deuterons.[49]

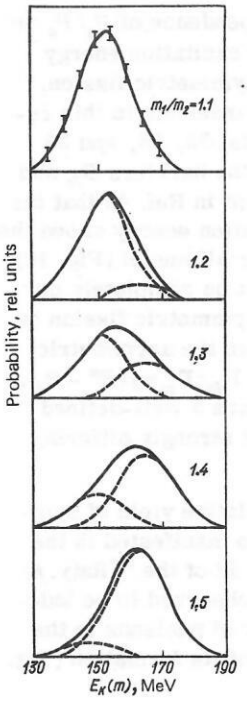

FIG. 14. Profiles of the kinetic energy distribution of the fragments for different mass ratios in ^{226}Ra fission by 12-MeV deuterons. The dashed curves are the assumed E_{ks} and E_{ka} distributions.[49]

distributions E_{ks} and E_{ka}. With increasing asymmetry of the fission, the symmetric distribution E_k went over into a distribution with prolonged high-energy decline and then again into a symmetric distribution at $m_1/m_2 \geqslant 1.5$. Such a change in the profile of the E_k distribution must be obtained if each of the superimposed distributions has a half-width greater than the distance between the most probable values of E_{ks} and E_{ka}.

In Refs. 56 and 57, one further attempt was made to separate the two types of fission on the basis of the number of neutrons $\nu(m)$ evaporated from fragments of different mass. By means of simultaneous measurement of the velocity and energy of pair fragments of ^{226}Ra(p,f) fission the calculation of $\nu(m)$ shown in Fig. 15 was made. It was found that a linear dependence of $\nu(m)$ of liquid-drop type corresponds to the peak of symmetric fission, in contrast to asymmetric fission. This distinctive dependence of $\nu(m)$ in the region of the symmetric peak appeared to support the hypothesis of two types of fission. However, it should be noted that such a profile of the $\nu(m)$ curve for Ra was predicted by Terrell[58] on the basis of the known $\nu(m)$ of heavier nuclei without recourse to the hypothesis of two types of fis-

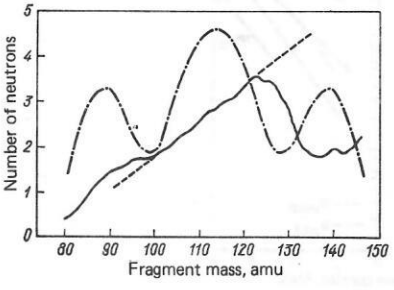

FIG 15. Yield of neutrons as a function of the mass of the fragment of ^{226}Ra fission by 13-MeV protons.[57] The chain curve is the mass yield curve of the fragments.

sion. A second feature of the neutron emission from the Ra fragments was that at $m = 130$, where the two putative types of fission are represented to an equal extent, an unusually strong dependence of ν on the total kinetic energy E_k of the fragments was observed. This could be a consequence of the fact that larger deformations of the fragments, i.e., small E_k and large ν, correspond to symmetric fission, whereas large E_k and small ν correspond to asymmetric fission. It was noted that the observed property cannot be readily explained by a specific property of only the fragments with $m = 130$, since it disappears, for example, in the spontaneous fission of californium. In similar measurements made at higher excitation,[59] the increase in the yield of the symmetric fission component qualitatively preserves the possibility of decomposing $\nu(m)$ into distributions of two types.

However, despite the listed arguments and the conviction of various authors that two types of fission really do exist,[48,60] the possibly physical origin of the phenomenon remained obscure. In addition, analysis shows that although the hypothesis can explain qualitatively the Ra–Ac characteristics, it fails for the fission of heavier nuclei. For example, one can make the following quantiative analysis of the position of the maximum of the $E_k(m)$ variance for fission of ^{232}Th by 12-MeV deuterons. The half-width of the mass distribution at the asymmetric fission peak, Δm_a, is approximately the same in the contour diagrams of radium,[49] thorium,[61,62] and uranium[63] ($\Delta m_a \approx 17$ amu). In the case of ^{232}Th fission by 12-MeV deuterons,[61] one can subtract from the $W(m)$ distribution the distribution of an asymmetric peak with half-width $\Delta M_a = 17$ amu. One then obtains a very narrow peak of the symmetric mass distribution with $\Delta m_c = 15$ amu (for radium, $\Delta m_c \approx 24$ amu). For such half-widths of the humps of symmetric and asymmetric fission, $\sigma^2[E_k(m)]$ must have its maximal value in the region of the mass $m_h = 125$ amu of the heavy fragment. But the maximum of the variance is observed at $m_h = 130$ amu. Decreasing the excitation of the nuclei by 3 MeV ($E_d = 9$ MeV) lowers the yield of symmetric fission fragments by a factor two.[61,62] It would seem that the variance is determined by the superposition of the distributions E_{ks} and E_{ka} and that its maximal value should be observed at even smaller ratios m_h/m_l ($m_h < 125$). Experimentally, such a tendency is not observed, and the position of the $\sigma^2[E_k(m)]$ peak remains as before. A similar discrepancy is observed when the other characteristics are analyzed quantitatively.

All this has had the result that although the hypothesis of two types of fission has not been proved to fail when applied to the Ra–Ac nuclei, the main attention is now directed toward an explanation of the triple-humped mass yield curve and other characteristics on the basis of the influence of the shell structure on the process of formation of the incipient fragments at all stages of fission, including scission.

Deformation Potential Energy of Radium and Actinium Nuclei and Calculation of the Fragment Mass Yield. We shall first of all consider calculations of the potential energy of nuclei as a function of the deformation with allowance for shell effects and pairing of the nucleons. After the appearance of Möller and Nilsson's paper,[64] it was clear that in the heavy post-thorium nuclei the potential energy at the second barrier is minimal in the case of asymmetric deformation. As a consequence, asymmetric fission of these nuclei can in a first approximation be formed at the second barrier and persist during the descent to the scission point.

The potential energy of the even radium isotopes was calculated similarly with allowance for shell effects and pairing of the nucleons as a function of the elongation of the nucleus and the degree of asymmetry.[34-36,43,44,65] Calculations using different forms of parametrization and analytic expression of the nuclear potential revealed the basic features of the deformation potential energy of ^{226}Ra and ^{228}Ra:

1) At the saddle point of the outer barrier asymmetric deformation with $m_1/m_2 = 1.2$–1.6 ($B_{fs} - B_{fa} = 1$–2 MeV) is favored.

2) Some calculations lead to a complicated form of the potential surface with a saddle or channel of symmetric fission and a lower saddle of asymmetric fission[35,36].

3) The asymmetric channel persists during the descent from the barrier to the scission point in the majority of the calculations.

Thus, the properties of the potential surface correspond qualitatively to the experimental mass distribution of the Ra–Ac fragments at low excitations.

The form of the potential surface of the deformation served as the basis for different types of quantitative calculation of the mass yield curve of the fragments. Tsang and Wilhelmy[66] used the simplest assumption that $W(m)$ at different excitations is determined at the outer barrier as proportional to the density of levels above the corresponding potential energy:

$$P_{fi} \sim \exp\left[2\sqrt{a\,(E^* - B_{fi})}\right], \quad i = a;\ s.$$

However, in such an approach it is impossible to explain the experimentally observed rapid growth of the symmetric hump with increasing excitation energy if one does not specify for this type of fission a higher density parameter of the levels ($a_s > a_a$). In particular, in Ref. 3 in an investigation of ^{228}Ra fission it was assumed that the growth of Γ_{fs} is due to nonaxial γ deformation.

Jensen and Dossing[67] obtained the density of levels for different excitations directly from a calculation of the density of single-particle states, and not from the Fermi-gas model. They assumed that the mass yield curve is formed somewhat after the saddle point. In calculations of this type for ^{226}Ra as a function of E^* a family of symmetric mass yield curves of the fragments was obtained with "influxes" of asymmetric fission of varying intensity that were not similar to the experimental curves. Closer to the experimental results was the calculated curve for the mean excitation of Ra when a term taking into account asymmetric vibrations was included in the Hamiltonian of the system during the descent from the barrier.[68]

Finally, for a sufficiently strong coupling between the single-particle and collective motions during the descent from the barrier the statistical method of calculating the probability of formation of different pairs of fragments at the scission point is justified. This method, which was proposed by Fong,[69] was developed to give reasonable agreement with the experimental characteristics of asymmetric fission of Th–Fe and symmetric fission of Po.[70-72] In the same category of investigations, in which it is assumed that the fragments are formed at the scission point, belongs the paper of Wilkins *et al.*[73] published in 1976. Besides calculating $W(m)$ of nuclei from Po to fermium, they devoted considerable attention to elucidating the properties of symmetric and asymmetric fission of radium. They assumed that during the descent from the barrier there is a strong coupling between the collective forms of motion, which are characterized by a temperature T_{coll}. The probability of formation of a given fragment pair was determined as

$$p(m_1, m_2) = \int_{\beta_1=0}^{\beta_{max}} \int_{\beta_2=0}^{\beta_{max}} \exp(-V/T_{coll})\, d\beta_1\, d\beta_2,$$

where $T_{coll} = 1$ MeV; V is the potential energy of the system at the scission point with allowance for the shell correction, the pairing of the nucleons, and the nuclear interaction between the ends of the elliptic fragments; and β is the quadrupole deformation parameter of the fragments ($\beta_{max} = 1$).

The shell correction in these calculations depended on the nucleon composition of the fragments, their deformation, and their internal excitation, characterized by the temperature T_{int} ($T_{int} \neq T_{coll}$). At medium excitation energies, the shell corrections resulted in a mass yield curve of the radium fragments with three humps (the dashed curve in Fig. 16), this having a qualitative resemblance to the experimental distribution. Generally, in the theoretical interpretation of symmetric and asymmetric fission of Ra, the most difficult problem is to explain the transition from the asymmetric distribution of the fragments at the barrier to the symmetric distribution at higher excitation. In the model calculation under consideration, it is noted that at the scission point the lowest potential energy is obtained for $m_h = 134$ (asymmetric fission) and is equal to the potential of the experimental barrier. It is then concluded that the

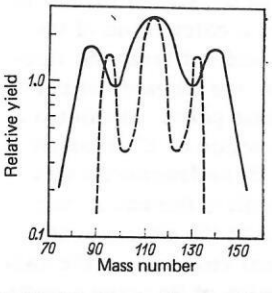

FIG. 16. Dependence of the mass yield of Ra fission fragments.[73] The continuous curve is from the experiment of Ref. 57 and the dashed curve is the result of the calculation of Ref. 73.

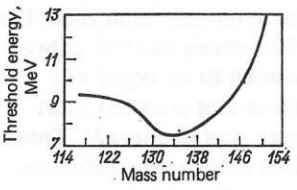

FIG. 17. Threshold energies of Ra fission for formation of different fragment masses. The calculated curve is taken from Ref. 73.

scission point and the saddle point coincide. Symmetric fission at the threshold is prevented by the higher potential barrier (Fig. 17), i.e., the fission must be asymmetric at the threshold. But, as is noted in Ref. 73, increasing the excitation energy reduces the shell corrections, or, for $T_{int} > 0.5$ MeV, reduces the potential energy of symmetric fission and raises the potential energy of asymmetric fission (Fig. 18). It therefore appeared that Wilkins *et al.* had explained from the point of view of statistical theory at the scission point the main features of Ra fission:

1) the height of the fission barrier as the lowest potential energy at the scission point, corresponding to $m_h = 134$;

2) the asymmetry of the mass distribution at the threshold;

3) the appearance of the triple-humped distribution at higher excitation as a consequence of the shell structure of the corresponding fragments;

4) the increase in the probability of symmetric fission with increasing excitation as the result of a decrease of the shell correction and the total potential energy of the system.

However, these calculations contain rather a lot of debatable elements, for example, the identification of the saddle point and the scission point. It follows from a number of calculations that the potential energy of the saddle point of not only radium,[34-36,43] but also the lighter nuclei Po (Ref. 74) and Pb (Ref. 75) is appreciably higher than the potential energy of the scission point. Their identification in Ref. 73 is evidently due to the rather approximate description of the shape of the fragments. In addition, the variation of the shell correction in Fig. 18 does not explain the experimental results for $T_{int} \leq 0.5$ MeV, since in this region of excitations the experimental yield of the symmetric fission component increases as rapidly as for $T_{int} > 0.5$ MeV.

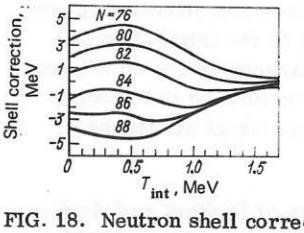

FIG. 18. Neutron shell correction to the potential energy of the liquid-drop model as a function of the internal excitation temperature.[73]

Mass Formation Phase of the Fragments. One of the main problems in understanding fission physics is the determination of the phase in which the mass distribution of the fragments is established. Despite important successes, this problem is still unsolved. When the asymmetric mass distribution of fission fragments of nuclei heavier than thorium is considered, it is sometimes assumed that to each fragment mass ratio m_1/m_2 there corresponds a definite degree of asymmetry at the second barrier, i.e., a particular height of the barrier, excitation, and set of projections K of the angular momentum onto the symmetry axis. This naive view of the formation of mass distributions is hardly justified. Allowance for the dynamics of the process includes the consideration for a given mass ratio of not one but a set of trajectories in the space of deformations, i.e., the set of shapes of the nuclei and excitation energies at the barrier. As an example of a dynamical calculation we can mention the determination by Pauli and Ledergerber[76] of the least-action integral for spontaneous fission of actinides as a function of the coordinate q of the separation and the potential $V(q)$ with shell correction:

$$s(q)=\int_{q}^{\cdot} dq \sqrt{|E-V(q)|\,2B_q(q)}.$$

The effective mass $B(q)$ was calculated in accordance with the cranking model. It was found that the trajectories of least action for different mass ratios of the fragments lie near the asymmetric saddle on the second barrier and diverge after the barrier during the descent. Thus, a trajectory which passes an asymmetric form on the barrier can even lead to symmetric mass separation in the fission of heavy nuclei. In this respect, Ref. 76 developed the suggestion made in Ref. 77 that the descent stage has a decisive influence on the formation of the mass yield. Similar views were expressed by Borisova *et al.*[78] on the basis of an experimental determination of the equality of the thresholds for symmetric and asymmetric fission ($B_{fs}=B_{fa}$) of ^{237}Np by neutrons. The conclusion that symmetric and asymmetric fission of heavy actinides passes through the same asymmetric saddle accords with the results of a number of experiments that measured the angular distribution of their fragments. According to the established ideas, the anisotropy of the expansion of the fragments is determined at the second barrier, and therefore identity of B_{fs} and B_{fa} leads as a consequence to the same anisotropy: $A_s=A_a$.[79-81]

The situation may be different for the triple-humped distribution of the Ra–Ac fragments. As we have noted above, calculation of the deformation potential energy surface by Strutinskiĭ's shell-correction method shows that these nuclei can have two saddle points. In the dynamical approach, different families (bunches) of trajectories that pass the second barrier through the symmetric and asymmetric saddle and overlap to only a slight extent can lead to the symmetric and asymmetric fission components. The fact that the symmetric component becomes appreciable in the experimental fission cross section at excitations 1.5–2 MeV higher than the threshold of asymmetric fission (see Figs. 8 and 9) would seem to confirm such an assumption. Another way of testing its validity is through experimental measurement of A_s and A_a at the fission threshold. A difference between the barrier heights B_{fs} and B_{fa} must lead to different sets of projections K_s and K_a of the total angular momenta onto the symmetry axis of the nuclei at the saddle point, i.e., to $A_s \neq A_a$. Several studies of this kind, which are called correlation experiments, have been made. Initially, they were made at comparatively high excitations above the barrier ($E^*-B_f>5$ MeV), and therefore the observed equality $A_s=A_a$ did not result in an unambiguous conclusion.[6] Then, using direct reactions, measurements were made in the immediate proximity of the fission threshold.[33,38,39] The authors of the quoted papers are inclined to assume that $A_s>A_a$. However, in my view their results do not have the necessary accuracy for such an assertion. The anisotropies A_s and A_a do differ to within the errors for ^{227}Ac and ^{228}Ac fission (see Fig. 9), but for ^{228}Ra (Ref. 33) and the light isotopes of thorium[50] A_s and A_a are equal.

One further measurement of this kind was made for fission of ^{226}Ra by 7.0-MeV neutrons, i.e., at 1 MeV and 3 MeV, respectively, above the assumed symmetric and asymmetric thresholds.[82] The symmetric and asymmetric fission components were separated on the basis of the kinetic energy spectra of the fragments at 0° and 90° to the neutron beam by means of the expression (3). The values of A_s and A_a were found to be equal to within the error of 25% (the measurements of Konecny *et al.*[38,39] had the same accuracy).

Let us estimate the restrictions that these data impose on the characteristics of the transition nucleus. The simple relation between the anisotropy of the fission and the variance of the distribution of the projection of the total angular momentum of the nucleus at the saddle point onto its symmetry axis (K_0^2) has the form

$$A=1+\bar{I}(\bar{I}+1)/4K_0^2\approx 1+\bar{I}^2/4K_0^2; \quad \bar{I}^2=(5.2)E_n, \tag{4}$$

where $\bar{I}$ is the mean angular momentum of the compound nucleus, and E_n is the energy of the neutrons. If we assume $A_a=A_s=A=1.5$ (Ref. 83), then an error in A_s of 25% will correspond to the restriction $|K_s|=3^{+2}_{-1}$, and for the asymmetric component we obtain $|K_a|=3$. The values of K_s and K_a are either equal or fairly close to each other. If they nevertheless differ and are due to different saddle points, then in accordance with the expression

$$K_0^2=TI_{\text{eff}}/\hbar^2\sim\sqrt{E^*-B_f}\,I_{\text{eff}}/\hbar^2 \tag{5}$$

the difference $K_{0s}^2-K_{0a}^2$ is determined by the difference between the effective moments of inertia and the fission barriers. The effective moments of inertia of the symmetric and the asymmetric configuration at low excitation energies are most accurately calculated in the superfluid model. For ^{227}Ra, there are no such data in the literature. In the analyzed experiment, the excitation of ^{227}Ra at the saddle point was appreciably lower than the critical value corresponding to the phase transition, but as a rough approximation the moments of inertia of the symmetric and the asymmetric configuration were taken in Ref. 82 to be equal to the rigid-body values and were nearly equal. In this rigid-body ap-

proximation, K^2_{0s} and K^2_{0a} could differ only by the corresponding temperatures. For the assumed difference $B_{fs} - B_{fa} = 2$ MeV, $K^2_{0a}/K^2_{0s} = 1.7$ is obtained from (5). This value is within the range of values admitted by the errors of the exerpimental A_s and A_a. Thus, if the physical conclusions are to be made more definite, it is necessary to increase the accuracy of the correlation experiments and also make a better calculation of the effective moments of inertia.

More definite results than those of correlation experiments using direct reactions or bombardment of Ra with neutrons were obtained in Refs. 51 and 52 in the ^{226}Ra(γ, f) reaction. In this case, the symmetric fission component becomes appreciable at limiting energy of the γ-ray bremsstrahlung spectrum at about 1.5 MeV above the threshold of asymmetric fission (see Fig. 11), i.e., one can assume that $B_{fs} - B_{fa} = 1.5$ MeV. In this respect, the photofission process is similar to other types of excitation. But there are fundamental differences: first, at the threshold, the anisotropy of photofission is several times greater than for fission induced by particles; second, because of the predominance of dipole absorption of the γ rays, the nuclei at the saddle point have a simple set of possible states with $I = 1^-$ and $K = 0^-, K = 1^-$. Because of this circumstance, the interpretation of the experiment is much simpler. The results of the measurement of the anisotropy of the symmetric and asymmetric fission is shown in Fig. 19 in the form of points with their statistical errors. If the outer potential barrier of the symmetric fission component is about 1.5 MeV higher than for the asymmetric component, then for otherwise identical characteristics the anisotropy curve of symmetric fission must be displaced with respect to the curve of the anisotropy of the expansion of the fragments (see Fig. 19a) by the same 1.5 MeV. The experimental points are systematically lower. It is improbable that the same energy dependence of the anisotropy of symmetric and asymmetric fission in the case of different barriers is due to the compensation of other characteristics such as the distance between the levels with $K = 0^-$ and $K = 1^-$ or the difference in the widths of the barriers. It is simpler and more plausible to assume that the same saddle point corresponds to the symmetric and asymmetric fission components. Then, as a consequence, their anisotropy is the same, and the relative probability, or the yield curves for them, are determined during the descent from the potential barrier to the scission point.

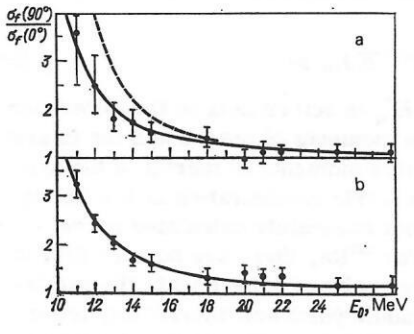

FIG. 19. Anisotropy of symmetric (a) and asymmetric (b) fission of ^{226}Ra as a function of the limiting energy of the γ-ray bremsstrahlung spectrum. The continuous curve is the anisotropy without the decomposition into components; the dashed curve is the same with displacement by 1.5 MeV.[52]

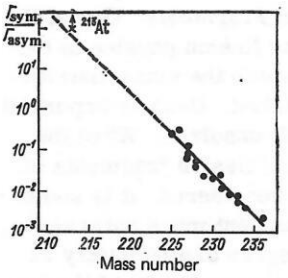

FIG. 20. Ratios of yields (widths) of symmetric and asymmetric fission as a function of the mass number of the compound nucleus at excitation of 2 MeV above the barrier. The black circles are from Ref. 87 and the crosses are for ^{213}At from Ref. 84.

The experiment on the fission of ^{213}At at the threshold of the ^{209}Bi$+\alpha \rightarrow {}^{213}At\rightarrow f$ reaction[84] has a direct bearing on the problem of elucidating the phase in the deformation of the intermediate nuclei at which the symmetric fission component is formed. As was noted above, it follows from the theoretical calculations of Pashkevich[75] and Mustafa *et al.*[74] that not only the elements after Th but also the fissile Po and Pb nuclei have a large asymmetric deformation at the saddle point. During the descent from the potential barrier, the Po and Pb nuclei must undergo an energetically advantageous (for them) symmetrization. A similar asymmetric deformation at the saddle point can be expected for ^{213}At, which is in the intermediate region. Complementing the already existing experimental data on the symmetric fission of At (Ref. 85), Po (Ref. 86), and lighter nuclei at medium excitation energies, the investigation of Ref. 84 into the kinetic energy spectrum of the fragments established that ^{213}At fissions symmetrically at even lower excitations ($E^* = B_f = 1$, 2, and 3 MeV), i.e., in the immediate proximity of the threshold. As can be seen from Fig. 20, the fraction corresponding to the symmetric fission component near the threshold increases rapidly with decreasing mass of the compound nucleus. A change of Z by only three units, from 85 to 88, leads to transition from symmetric fission at the At threshold to asymmetric fission of Ra. Thus, if asymmetric deformation really does correspond to the second barrier for nuclei in the region of At, this leads to a general picture of the formation of the symmetric fission component during the descent from the barrier for not only Ra–Ac but also the lighter nuclei At–Po–Pb.

At the present time, this picture of symmetric fission cannot be regarded as definitively established. There is an alternative scheme, in which one adopts the following assumptions:

1) To the experimental symmetric fission of Pb, Po, and At there corresponds a symmetric shape at the saddle point, as is obtained, for example, in Möller's calculations.

2) The deformation potential energy surface of Ra–Ac

has symmetric and asymmetric saddles with corresponding $B_{fs} > B_{fa}$. This explains why Ra and Ac fission asymmetrically at the threshold, and with increasing excitation the rapid growth of the symmetric yield through the symmetric saddle is due to the large density parameter of the levels ($a_s > a_a$). Recently, this point of view has been advocated in Refs. 33, 38, and 39. However, as we have noted earlier, this scheme does not agree with the equality of the anisotropy of symmetric and asymmetric fission, which is manifested particularly clearly in the ^{226}Ra(γ, f) reaction.

To establish the true picture, we need further experiments and theoretical calculations taking into account dynamical effects during the descent from the potential barrier between the saddle point and the scission point.

Unfortunately, the experimental technique does not permit measurements at the descent times ~10^{-20} sec from the barrier presupposed in the theory. It is therefore very desirable to develop the correlation experiments in the direction of increasing accuracy in the measurement of the anisotropy of the symmetric and asymmetric component for different types of excitation of the Ra and Ac nuclei. In particular, a search for a quadrupole component in the angular distribution of the fragments of symmetric photofission in the region of excitations of the putative threshold would enable one to draw conclusions about the asymmetry of the nucleus at the corresponding saddle points. If a preferential yield of fragments at angle 45° were found, this would indicate a difference between the heights of the levels with $K = 0^+$ and $K = 0^-$, i.e., a symmetric shape of the nucleus at the saddle point.[40,88]

A new source of information on the properties of symmetric and asymmetric fission could be obtained by bombarding radium with electrons at energy close to the fission threshold. In contrast to the ordinary predominant dipole absorption of photons, the excited even-even ^{226}Ra nuclei formed in this case will, after absorption of virtual γ rays, be in $I = 1^-$ and $I = 2^+$ states in comparable numbers. The high percentage of fission events with $(I, \pi, K) = (2, +, 0)$ and its inherent preferential yield of fragments at 45° to the direction of the electron beam will provide the basis for obtaining additional information about the shape of the nucleus at the saddle point.

3. ANGULAR DISTRIBUTION OF FRAGMENTS AND CHARACTERISTICS OF THE NUCLEAR STATES AT THE FISSION BARRIER

The experimental measurement of the angular distribution of the fragments has proved to be an extremely effective means for investigating the properties of strongly deformed nuclei. This approach has yielded the characteristics of individual low-lying levels of the nuclei in the transition state and the averaged characteristics for high excitations. As in other fields of experimental investigation of fission, work on the angular distribution of fragments at the threshold has been done until recently on nuclei with $Z \geq 90$. From the point of view of the latest descriptions of the fission barrier in the form of a double-humped curve, the determination of the characteristics of the channels of the transition nuclei of Ra could be a very interesting "pure" case. Whereas for nuclei with $Z \geq 90$ the levels at the second barrier are hard to separate from the levels in the potential well of the isomer state, the radium barrier can on the basis of theoretical studies[35,65] be regarded as effectively single-humped, and then only channels above the second barrier affect $W_f(\theta)$. But of course these advantages will not be realized if in Ra and Ac the outer barrier is split into two humps, as in the case of the light isotopes of thorium.[44] Up to the present time, papers have been published reporting measurement of the fragment angular distributions resulting from bombardment of Ra with γ rays, neutrons, and charged particles.

Photofission. Photofission of even-even nuclei is the simplest case in the channel analysis of the fragment angular distribution. The predominant dipole absorption of the γ rays for zero spin of the even-even target nucleus leads to a unique value of the angular momentum $I = 1^-$, projections $M = \pm 1$ onto the direction of the γ-ray beam, and projections $K = 0, K = 1$ of the angular momentum onto the symmetry axis of the nucleus. The total angular distribution of the fragments with allowance for the small contribution of quadrupole absorption of the γ rays is determined by the expression

$$W_f(\theta) = a + b \sin^2\theta + c \sin^2 2\theta.$$

Angular distributions of the fragments were obtained in the range of variation of the limiting energy E_0 from 9.1 to 26 MeV when ^{226}Ra was irradiated with bremsstrahlung γ rays from high-current accelerators.[22] The properties of the distributions and the conclusions drawn from them are as follows.

1. As in the fission of other even-even nuclei, there is predominant emission of fragments at 90° to the γ-ray beam. The anisotropy decreases with increasing E_0.

2. The experimental $W_f(\theta)$ curves have a monotonic form without any local increases in the yield between 0° and 90°. There is no justification for including a quadrupole term at any E_0, i.e., the distributions have the form

$$W_f(\theta) = a + b \sin^2\theta \sim 1 + \alpha \sin^2\theta.$$

To the values $E_0 = 9.1$, 10.7, 14.5, 18, 22, and 26 MeV there correspond the anisotropy coefficients $\alpha = 6$, 2.3, 0.65, 0.34, 0.16, and 0.08.

3. The lowest value $E_0 = 9.1$ MeV exceeds the ^{226}Ra fission barrier by approximately 0.6 MeV. In the case of analogous above-barrier excitation the presence of quadrupole fission in the fragment angular distribution of ^{240}Pu photofission leads to $c/b = 0.3$–0.9. In the case of radium photofission, $c/b \leq 0.07$. The absence of quadrupole fission can be attributed to the outer hump of the Ra barrier being higher than the inner hump ($B_{f2} > B_{f1}$), this corresponding to asymmetric deformation of the nucleus at the saddle point. In such a case, as in the photofission of ^{232}Th, the asymmetric deformation leads to degeneracy of the levels with $K = 0^+$ and $K = 0^-$,

i.e., to the effective absence of a quadrupole term in the angular distribution of the fragments at the photofission threshold.[40,88] To increase the reliability of the conclusions about the asymmetric deformation of Ra at the saddle point, it is desirable to continue the measurement of $W_f(\theta)$ at $E_0 < 9$ MeV.

4. Having established in our institute in Ref. 22 that the photofission of ^{226}Ra occurs basically after the dipole absorption of the γ rays in the complete investigated E_0 range, we determined the difference of the excitation energies between the states with $(I, \pi, K) = (1, -, 0)$ and $(I, \pi, K) = (+, -, 1)$. The calculations was based on the method proposed by Baerg *et al.*[89] It was assumed that the Ra barrier is parabolic and that its penetrability is determined by Eq. (1). On the basis of the modern picture of a double-humped barrier of heavy nuclei, the following distances were obtained for ^{226}Ra, ^{232}Th, ^{238}U, and ^{240}Pu between the $K = 0^-$ and $K = 1^-$ levels at the saddle point: 0.45, 0.32, 0.3, and 0.17 MeV. In the calculation for Th, U, and Pu, the values of the potential barriers and their curvature parameters were taken from Ref. 90. As can be seen from the comparison, the distance between the levels with $K = 0^-$ and $K = 1^-$ decreases with Z and A of the fissioning nucleus.

According to existing ideas, at low excitations $K = 0^-$ characterizes octupole vibrations and $K = 1^-$ characterizes bending vibrations (Fig. 21). At deformations corresponding to the ground states, the level with $K = 0^-$ is lowest in Ra. Evidently, this is also true of the listed nuclei at the saddle point, which means that Ra has the greatest distance between $K = 0^-$ and 1^-.

Above, we have noted the desirability of experiments on the electron fission of Ra. Measurement of the angular distributions of the fragments at the fission threshold in this case could give additional spectroscopic information about the relative position of the level at the saddle point with $K = 0^+$.

Fission of Radium by Neutrons. Experiments to measure the angular distribution of fragments from Ra fission by neutrons have been made over a wide range of energies E_n from threshold values to 20 MeV (Fig. 22).[11,12,37,44,83] According to the specific physics of the

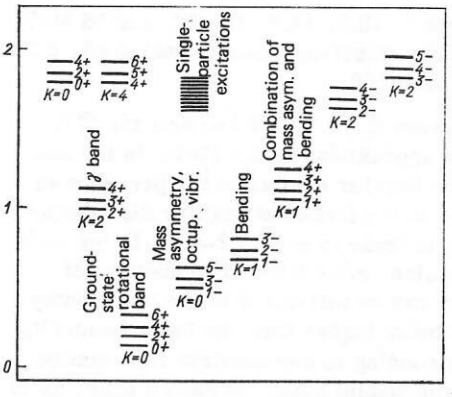

FIG. 21. Level scheme of even–even nucleus for stable quadrupole deformation.[40]

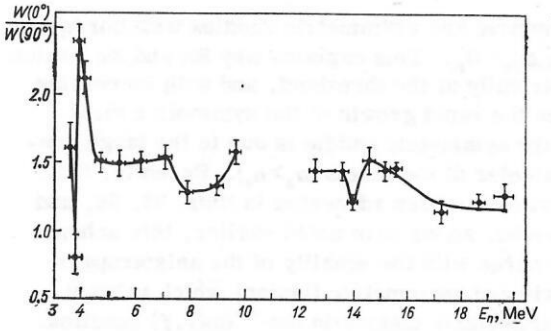

FIG. 22. Energy dependence of the angular anisotropy of the fragments of ^{226}Ra fission by neutrons.[11,12,37,83]

reaction, the analysis of the results can be divided into three regions: 1) excitations near the fission barrier; 2) the region of E_n up to the onset of emission fission, i.e., up to $E_n = 9$ MeV; 3) the region of excitations in which a contribution of the $(n, n'f)$ and $(n, 2n'f)$ reactions is observed in the fission.

Measurements of $W_{n,f}(\theta)$ at the barrier correspond to essentially more varied states of the transition nucleus compared with the ^{226}Ra(γ, f) fission described above. Channel effects in the angular distribution of the fragments have been observed by a number of investigators in the fission of ^{230}Th, ^{232}Th, ^{234}U and other nuclei by neutrons. The complicated $W_f(\theta)$ profile is attributed to the quantum numbers of the discrete levels of the listed nuclei at the outer barrier and in the second potential well. As the measurements showed, the channel effects manifested in the complicated $W_{n,f}(\theta)$ profile and the rapid variation of the anisotropy $A = W_f(0°)/W_f(90°)$ when E_n varies in the region of the threshold by about 0.1 MeV are also observed in the ^{226}Ra(n, f) reaction (see Fig. 22). Decomposing the experimental curves into Legendre polynomials and comparing them with the profiles of the theoretical angular distributions of the fragments for different I and K combinations,[91] Babenko *et al.*[12] found that at the ^{227}Ra fission barrier the levels with $K = 1/2$ and $3/2$ are most strongly manifested. Using the same experimental data on $W_{n,f}(\theta)$ and $\sigma_{n,f}$, Groening and Loveland[92] made a more detailed channel analysis. In addition to the above states, they noted the influence of a level with $K = 5/2$. In their calculations, Groening and Loveland assumed that the ^{227}Ra fission barrier has a single-humped parabolic shape. However, there have recently appeared serious arguments in favor of a more complicated structure of the outer barrier of the light actinides. As was noted above, the calculations of Möller and Nix[44] revealed a splitting of the second hump of the fission barriers of the light thorium isotopes, this making it possible to explain the so-called *anomalous vibrational resonances* in $\sigma_{n,f}$(Th). Such calculations have not yet been made for radium, but the resonance in the excitation function at the ^{228}Ra fission threshold is attributed by Konecny *et al.*[33] to the presence of a vibrational level in the third potential well, which has depth ~1 MeV. In the case of splitting of the second hump in ^{227}Ra, the experimental channel structure of $W_{n,f}(\theta)$ in the ^{226}Ra(n, f) reaction at the fission threshold could be due to levels in the third potential well.

In the region $E_n = 4-9$ MeV, the angular distribution of the fragments is described by the expression

$$W_{n,f}(\theta) = a + b\cos^2\theta,$$

i.e., it corresponds to a statistical distribution of K. Using the formula

$$A = (2.1\sqrt{E_n}+1)^2/8K_0^2+1$$

of Ref. 93, the variance K_0^2 of the distribution was calculated (Fig. 23) on the basis of the experimental anisotropy A. For $E_n = 5-7$ MeV, the variance is hardly changed, forming a step at the level $K_0^2 \approx 9$. This step variation of K_0^2 is usually interpreted as due to a manifestation of discreteness in the change in the number of excited quasiparticles. By means of the formula for the threshold of the n-quasiparticle state[94]:

$$U_{n,\min} = n\Delta\,(1 - n\,2g\Delta)$$

the value $\Delta_f(^{227}\mathrm{Ra}) = 0.9-1.0$ MeV was obtained, i.e., a value close to the correlation function of the ground state of the undeformed heavy nucleus. In such an approach, to the initial one-quasiparticle state at the potential barrier there corresponds $K_0^2 = 3-4$; the rise in K_0^2 at $(E^* - B_f) \approx 1.1$ MeV is due to the three-quasiparticle state, and the second rise at $(E^* - B_f) \approx 3.5$ MeV is due to the five-quasiparticle state. The $K_{01}^2 : K_{02}^2 : K_{03}^2$ ratio is found to be close to the theoretical ratio 1:3:5. Earlier, a step structure of K_0^2 at the fission barrier was observed both in heavy transuranium elements[95] and in the fission of pre-actinide nuclei.[96]

In the model of a superfluid nucleus, the discrete change in the number of excited quasiparticles leads to steps at the barrier not only in K_0^2 but also in the level density of the nucleus, i.e., in Γ_f. In this connection, it is interesting to note the small step in $\sigma_f(^{226}\mathrm{Ra}+n)$. The energy at which the fission cross section makes the second step up ($E_n = 4.8-4.9$ MeV) coincides with the first step in K_0^2. The observed correlation is an argument in favor of regarding it as a three-quasiparticle excitation.

Thus, the changes in the anisotropy of the angular distribution of the Ra fragments, K_0^2, and $\sigma_{n,f}(^{226}\mathrm{Ra})$ can be satisfactorily described by the superfluid model. We must not fail to draw attention to the fact that this agreement is of the nature of a first approximation. Because of the difficulty of the experiment, the accuracy of the measurement is low, and continuation of the experiments on fission by neutrons of the intermediate nuclei would provide much useful material.

At $E_n = 9.7$ MeV, the anisotropy is increased because of the onset of emission fission. The increase is less pronounced than for the actinide nuclei. An explanation for this is that in Ra the ratio Γ_f/Γ_n increases rapidly with increasing excitation and, therefore, the addition to σ_f from emission fission does not take place abruptly but in a smooth increase. The profile of the angular distributions of the fragments at $E_n = 14.6-15.6$ MeV (Fig. 24) was found to be unusual when compared with the $W_f(\theta)$ of heavier nuclei. This means that in the given E_n range the distribution of the K values is not statistical. Individual "channels" with definite K can be manifested only by cooling the nucleus at the saddle point to excitations near the fission barrier, i.e., by evaporation from the compound nucleus of two neutrons before fission. The angular distribution of the fragments has a complicated profile in a fairly wide range of E_n. The increased excitation of the compound nuclei is apparently compensated by the fact that the corresponding fraction of emission neutrons carries away greater energy, and some of the nuclei remain as before with excitation near the fission barrier. A channel structure in the energy dependence of the anisotropy of the fission fragments at $E_n = 15-16$ MeV was also observed in the $^{232}\mathrm{Th}(n, 2n'f)$ reaction.[97]

Fission of Radium and Actinium by Charged Particles. As we noted above, the Coulomb barrier prevents formation of nuclei with low excitation. The angular distribution of the fission fragments of the actinides is in this case a superposition of the distributions belonging to fission of the initial, maximally excited compound nucleus and nuclei with excitation reduced by prior emission of neutrons. The superposition of the distributions complicates the analysis and the extraction of

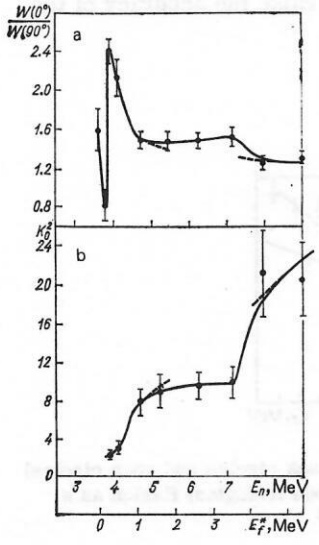

FIG. 23. Anisotropy of the angular distribution of fragments from ^{226}Ra fission by neutrons and K_0^2 as functions of the excitation energy above the barrier and the neutron energy.[83]

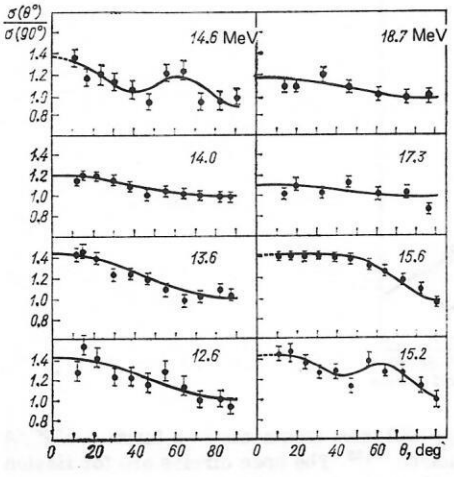

FIG. 24. Angular distributions of fragments from ^{226}Ra fission by neutrons with energy 12–19 MeV.[37]

information about characteristics of the nucleus at the saddle point such as K_0^2 and I_{eff}.

The main features of the angular distributions of the fragments from the fission of heavy nuclei by charged particles are as follows:

1) The distributions have a smooth profile with monotonic increase in the fragment yield at 0° and 180° relative to the direction of the beam of charged particles.

2) The anisotropy is relatively greater when the nuclei are bombarded with particles of greater mass, which impart a larger angular momentum to the compound nucleus (Fig. 25). In particular, bombardment with protons leads to an almost isotropic angular distribution of the fragments.

3) In a first approximation, the anisotropy of the angular distribution decreases with increasing Z^2/A of the target nuclei. However, in the region of Ra a departure from this fairly smooth dependence is observed. Such a departure was noted, for example, in the case of fission by 21-MeV deuterons[98] and 42.8-MeV α particles[99] (see Fig. 25).

The properties noted under 1) and 2) are fully manifested in the measured angular distributions of the fragments of Ra fission by protons,[6,7] deuterons,[5,7,9] and α particles[5] and Ac fission by deuterons.[10]

Let us consider in more detail the "anomalous" decrease in the anisotropy of the Ra fission fragments noted in 3) and in Fig. 25. In the region of nuclei with $Z \geq 90$, a decrease in Z^2/A is accompanied by an increase in the post-emission, cooled fission. The height of the outer barrier is also raised. Both of these factors reduce the mean temperature of the nuclei, i.e., they increase the anisotropy. At the intermediate Ra and Ac nuclei, there is an appreciable increase in B_f. This abrupt increase reduces the probability of emission fission, increases the effective temperature of the nuclei at the saddle point, and decreases relatively the anisotropy. For nuclei with $Z \leq 85$, emission fission is virtually absent at the considered excitations. Only the growth of B_f influences the temperature ($T \sim \sqrt{E^* - B_f}$), and the anisotropy again increases with decreasing Z^2/A. Bombarding nuclei with α particles shifts the point of inflection in the anisotropy curve (see Fig. 25), since capture of an α particle by Ra leads to the formation of ^{230}Th, which is identical to the heavier actinides.

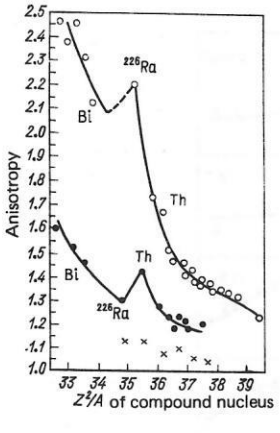

FIG. 25. Anisotropy of fission fragments as a function of Z^2/A of the compound nucleus.[98,99] The open circles are for fission by α particles, the black circles for fission by deuterons, and the crosses for fission by protons.

It can be seen from Fig. 26 (Ref. 9) that the difference between the Th and Ra anisotropy gradually disappears with decreasing deuteron energy. In particular, analysis shows that in the ^{226}Ra(d,f) and ^{232}Th(d,f) reactions at $E_d = 7$ MeV all the parameters determining the anisotropy are approximately equal:

1) The angular momenta introduced by the deuterons are small and have $l_{max} = 2$–3 (in the majority of cases, the fission is preceded by complete capture of a deuteron[9,61,100].

2) The excitations above the fission barriers are 8 and 9.4 MeV.

3) At these excitations close to the critical energy of the phase transition, the effective moments of inertia of the considered compound nuclei can be regarded as rigid-body moments and differing little.

4) In both cases, the fraction corresponding to emission fission is ~50%, i.e., the mean temperatures are also similar.

In this connection, it is natural that the experimental anisotropy in the fragment distribution from Ra and Th fission by 7-MeV deuterons should be the same. With regard to high excitations, the relative decrease of $A(^{226}\text{Ra} + d)$ compared with thorium fission can be explained by the smaller emission fission fraction, i.e., the higher mean temperature.

It would be worthwhile to investigate the angular distribution of fragments using direct reactions preceding fission: (d,p,f), (t,p,f), etc. Investigations of this kind with measurements of the anisotropy of the fragments of Ra and Ac nuclei near the fission threshold were made by Konecny *et al.*[33,38,39] They observed the usual averaged tendency for the anisotropy to decrease with increasing excitation energy of the nuclei. However, to obtain information about the structure of the barriers, it is necessary to raise the accuracy of the measurements.

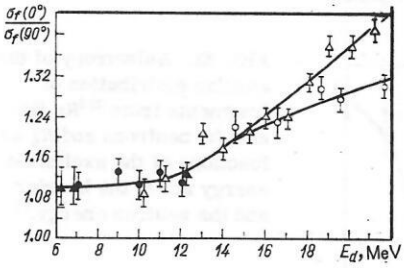

FIG. 26. Anisotropy of ^{226}Ra (black circles and open circles) and ^{232}Th (black triangles and open triangles) fission as a function of the deuteron energy.[9]

CONCLUSIONS

Varied investigations have now been made in the region of the nuclei with the unusual triple-humped mass distribution of the fragments. The main characteristics of the fission of Ra and Ac isotopes have been obtained: the fission cross sections and thresholds, the angular distributions of the fragments, their kinetic energies, the emission of neutrons from fragments of different mass, and the dependence of the fragment mass yield on the excitation energy. However, the comparatively low fissility of nuclei in the region of Ra–Ac, their intense α and γ radiation, and the separation of emanation have hitherto prevented the carrying out of experiments with the desired accuracy and detail. For example, an increase in the accuracy of the measurement of the total and differential fission cross sections at the threhold would make it possible to determine more precisely the profile of the barrier and to establish whether there really is a splitting of its second potential hump. The mechanism of formation of the triple-humped mass distribution of the fragments would be considerably clarified if new information could be obtained about the nature of the emission of neutrons from the fragments—their angular distribution, spectrum, and the value of $\nu(m)$ at different excitation energies or for different relative probability of symmetric and asymmetric fission.

It has recently been established that the triple-humped distribution of the mass yield curve of the intermediate nuclei cannot be explained by simple superposition of emissionless and emission fission. The three humps reflect a deeper property of nuclei with a definite nucleon composition and definite excitation. The main task of subsequent investigations will be to establish with confidence whether the symmetric fission component is formed at the barrier or during the descent to the scission point.

In conclusion, we can confidently say that the continuation of the investigation into the specific properties of Ra and Ac will yield additional new material necessary for the development of the complete theory of fission.

[1]R. C. Jensen and A. W. Fairhall, Phys. Rev. **109**, 942 (1958).
[2]R. C. Jensen and A. W. Fairhall, Phys. Rev. **118**, 771 (1960).
[3]R. B. Duffield, R. A. Schmitt, and R. P. Sharp, in: Proc. Second Intern. Conf. PUAE, Vol. 15, Geneva (1958), p. 202.
[4]R. A. Nobles and R. B. Leachman, Nucl. Phys. **5**, 211 (1958).
[5]J. E. Gindler, G. L. Bate, and J. R. Huizenga, Phys. Rev. B **136**, 1333 (1964).
[6]E. Konecny and H. W. Schmitt, Phys. Rev. **172**, 1226 (1968).
[7]D. G. Perry and A. W. Fairhall, Phys. Rev. C **4**, 977 (1971).
[8]B. J. Bowles and N. Beckett, Phys. Rev. **147**, 852 (1966).
[9]A. S. Dovgilenko *et al.*, Yad. Fiz. **5**, 538 (1967) [Sov. J. Nucl. Phys. **5**, 382 (1967)].
[10]V. A. Nikolaev *et al.*, Yad. Fiz. **19**, 751 (1974) [Sov. J. Nucl. Phys. **19**, 382 (1974)].
[11]Yu. A. Babenko *et al.*, Yad. Fiz. **7**, 269 (1968) [Sov. J. Nucl. Phys. **7**, 186 (1968)].
[12]Yu. A. Babenko *et al.*, Yad. Fiz. **10**, 233 (1969) [Sov. J. Nucl. Phys. **10**, 133 (1970)].
[13]E. A. Zhagrov *et al.*, Preprint RI-4 [in Russian], Radium Institute (1972).
[14]E. A. Zhagrov *et al.*, Nucl. Phys. **A213**, 436 (1973).
[15]I. M. Kuks *et al.*, Yad. Fiz. **22**, 934 (1975) [Sov. J. Nucl. Phys. **22**, 486 (1975)].
[16]O. V. Rumyantsev, Yu. A. Selitskiĭ, and V. B. Funshteĭn, Prib. Tekh. Eksp. No., 51 (1968).
[17]J. Stehn *et al.*, Neutron Cross Sections, BNL-325 (1965).
[18]H. Nakahara *et al.*, J. Inorg. Nucl. Chem. **36**, 487 (1974).
[19]I. M. Kuks *et al.*, Yad. Fiz. **24**, 1258 (1976) [Sov. J. Nucl. Phys. **24**, 659 (1976)].
[20]H. Nakahara *et al.*, J. Inorg. Nucl. Chem. **38**, 203 (1976).
[21]R. S. Iyer *et al.*, in: Proc. Symposium on the Physics and Chemistry of Fission, Salzburg, 1965, Vol. 1, IAEA, Vienna (1963), p. 439.
[22]E. A. Zhagrov, Yu. A. Nemilov, and Yu. A. Selitskiĭ, Yad. Fiz. **7**, 264 (1968) [Sov. J. Nucl. Phys. **7**, 183 (1968)].
[23]E. A. Zhagrov *et al.*, Yad. Fiz. **13**, 934 (1971) [Sov. J. Nucl. Phys. **13**, 537 (1971)].
[24]M. Danos, Nucl. Phys. **5**, 23 (1958).
[25]Yu. F. Nemets and Yu. V. Gofman, Spravochnik po yadernoĭ fizike (Handbook of Nuclear Physics), Naukova Dumka, Kiev (1975).
[26]H. C. Jain *et al.*, J. Inorg. Nucl. Chem. **29**, 267 (1967).
[27]P. del Marmol, F. Hanappe, and M. Monsecour, J. Inorg. Nucl. Chem. **35**, 4323 (1973).
[28]D. L. Hill and J. A. Wheeler, Phys. Rev. **89**, 1102 (1953).
[29]V. M. Strutinskiĭ, Yad. Fiz. **3**, 614 (1966) [Sov. J. Nucl. Phys. **3**, 449 (1966)].
[30]V. M. Strutinsky, Nucl. Phys. **A122**, 1 (1968).
[31]G. D. James, J. E. Lynn, and L. G. Earwaker, Nucl. Phys. **A189**, 225 (1972).
[32]W. D. Myers and W. J. Swiatecki, Nucl. Phys. **A81**, 1 (1966).
[33]J. Weber *et al.*, Phys. Rev. C **13**, 2413 (1976).
[34]V. M. Strutinskiĭ *et al.*, Preprint KIYaI-73-1Ya [in Russian].
[35]P. Möller, Nucl. Phys. **A192**, 529 (1972).
[36]H. C. Pauli, Phys. Rep. **C7**, 35 (1973).
[37]Yu. A. Babenko *et al.*, Yad. Fiz. **11**, 1006 (1970) [Sov. J. Nucl. Phys. **11**, 560 (1970)].
[38]E. Konecny, H. J. Specht, and J. Weber, Phys. Lett. **B45**, 329 (1973).
[39]E. Konecny, H. J. Specht, and J. Weber, in: Proc. Third Symposium on the Physics and Chemistry of Fission, Rochester, 1973, Vol. 2, IAEA, Vienna (1974), p. 3.
[40]R. Vandenbosch and J. R. Huizenga, Nuclear Fission, New York (1973).
[41]H. Freiesleben, H. C. Britt, and J. R. Huizenga, in: Proc. Third Symposium on the Physics and Chemistry of Fission, Rochester, 1973, IAEA, Vienna (1974).
[42]H. C. Pauli and T. Ledergerber, Nucl. Phys. **A175**, 545 (1971).
[43]G. D. Adeev, Dissertatsiya (Dissertation), Tomsk (1972).
[44]P. Möller and J. R. Nix, in: Proc. Third Symposium on the Physics and Chemistry of Fission, Rochester, 1973, Vol. 1, IAEA, Vienna (1974), p. 103.
[45]I. M. Kuks *et al.*, Yad. Fiz. **16**, 438 (1972) [Sov. J. Nucl. Phys. **16**, 244 (1973)].
[46]A. Gavron, H. C. Britt, and J. B. Wilhelmy, Phys. Rev. C **13**, 2577 (1976).
[47]B. B. Back *et al.*, Phys. Rev. C **10**, 1948 (1974).
[48]H. C. Britt, H. E. Wegner, and J. C. Gursky, Phys. Rev. **129**, 2239 (1963).
[49]Yu. A. Nemilov *et al*, Yad. Fiz **3**, 1070 (1966) [Sov. J. Nucl. Phys. **3**, 782 (1966)].
[50]H. J. Specht, Phys. Scr. **A10**, 21 (1974).
[51]E. A. Zhagrov *et al.*, Pis'ma Zh. Eksp. Teor. Fiz. **20** (1974) [JETP Lett. **20**, 95 (1974)].
[52]E. B. Bazhanov *et al.*, Yad. Fiz. **22**, 36 (1975) [Sov. J. Nucl. Phys. **22**, 17 (1975)].

[53]A. Turkevich and J. B. Niday, Phys. Rev. **84**, 52 (1951).
[54]G. P. Ford, Phys. Rev. **118**, 1261 (1960).
[55]H. B. Levy *et al.*, Phys. Rev. **124**, 544 (1961).
[56]H. W. Schmitt and E. Konecny, Phys. Rev. Lett. **16**, 1008 (1966).
[57]E. Konecny and H. W. Schmitt, Phys. Rev. **172**, 1213 (1968).
[58]J. Terrell, Phys. Rev. **127**, 880 (1962).
[59]Z. Fraenkel *et al.*, Phys. Rev. C **12**, 1809 (1975).
[60]H. Baba and S. Baba, Nucl. Phys. **A175**, 199 (1971).
[61]Ya. A. Nemilov *et al.*, Yad. Fiz. **1**, 633 (1965) [Sov. J. Nucl. Phys. **1**, 453 (1965)].
[62]Yu. A. Selitskiĭ, S. M. Solov'ev, and V. P. Éismont, Yad. Fiz. **3**, 65 (1966) [Sov. J. Nucl. Phys. **3**, 46 (1966)].
[63]Yu. A. Selitskiĭ, S. M. Solov'ev, and V. P. Éismont, Yad. Fiz. **3**, 868 (1966) [Sov. J. Nucl. Phys. **3**, 638 (1966)].
[64]P. Möller and S. G. Nilsson, Phys. Lett. **B31**, 283 (1970).
[65]G. D. Adeev, N A. Gamalya, and P. A. Cherdantsev, Izv. Akad. Nauk SSSR, Ser. Fiz. **36**, 644 (1972).
[66]C. F. Tsang and J. B. Wilhelmy, Nucl. Phys. **A184**, 417 (1972).
[67]A. S. Jensen and T. Dossing, in: Proc. Third Symposium on the Physics and Chemistry of Fission, Rochester 1973, Vol. 1, IAEA, Vienna (1974), p. 409.
[68]J. Maruhn and W. Greiner, Phys. Rev. Lett. **32**, 548 (1974).
[69]P. Fong, Phys. Rev. **102**, 434 (1956).
[70]A. V. Ignatyuk, Yad. Fiz. **7**, 1043 (1968) [Sov. J. Nucl. Phys. **7**, 626 (1968)].
[71]A. V. Ignatyuk, Yad. Fiz. **9**, 357 (1969) [Sov. J. Nucl. Phys. **9**, 208 (1969)].
[72]V. A. Rubchenya, Yad. Fiz. **9**, 1192 (1969) [Sov. J. Nucl. Phys. **9**, 697 (1969)].
[73]B. D. Wilkins, E. P. Steinberg, and R. R. Chasman, Phys. Rev. C **14**, 1832 (1976).
[74]M. G. Mustafa, U. Mosel, and H. W. Schmitt, Phys. Rev. C **7**, 1519 (1973).
[75]V. V. Pashkevich, Nucl. Phys. **A169**, 275 (1971).
[76]T. Ledergerber and H. C. Pauli, Nucl. Phys. **A207**, 1 (1973).
[77]U. Mosel and H. W. Schmitt, Nucl. Phys. **A165**, 73 (1971).
[78]N. I. Borisova *et al.*, Yad. Fiz. **2**, 243 (1965) [Sov. J. Nucl. Phys. **2**, 173 (1966)].
[79]B. D. Kuz'minov andA. I. Sergachev, in: Proc. Symposium on the Physics and Chemistry of Fission, Salzburg, 1965, Vol. 1, IAEA, Vienna (1966), p. 611.
[80]R. Vandenbosch, J. P. Unik, andJ. R. Huizenga, in: Proc. Symposium on the Physics and Chemistry of Fission, Salzburg, 1965, Vol. 1, IAEA, Vienna (1966), p. 547.
[81]J. W. Meadows, Phys. Rev. **177**, 1817 (1969).
[82]N. P. D'yachenko *et al.*, Yad. Fiz. **24**, 17 (1976) [Sov. Nucl. Phys. **24**, 8 (1976)].
[83]V. T. Ippolitov *et al.*, Yad. Fiz. **14**, 939 (1971) [Sov. J. Nucl. Phys. **14**, 526 (1972)].
[84]I. M. Kuks *et al.*, Preprint RI-51 [in Russian], Radium Institute (1976); Yad. Fiz. **27**, 54 (1978) [Sov. J. Nucl. Phys. **27**, 28 (1978)].
[85]M. G. Itkis *et al.*, At. Energ. **34**, 133 (1973).
[86]F. Plasil *et al.*, Phys. Rev C **7**, 1186 (1973).
[87]H. J. Specht, in: Seventh Polish Summer School on Nuclear Physics (1974).
[88]R. Vandenbosch, Phys. Lett. **B45**, 207 (1973).
[89]A. P. Baerg *et al.*, Can. J. Phys. **37**, 1418 (1959).
[90]A. V. Ignatyuk *et al.*, Zh. Eksp. Teor. Fiz. **61**, 1284 (1971) [Sov. Phys. JETP **34**, 684 (1972)].
[91]H. W. Lamphere, Nucl. Phys. **38**, 561 (1962).
[92]H. Groening and W. Loveland, in: Proc. Third Symposium on the Physics and Chemistry of Fission, Rochester, 1973, IAEA IAEA, Vienna (1974).
[93]V. G. Nesterov, G. N. Smirenkin, and A. S. Tishin, Yad. Fiz. **6**, 761 (1967) [Sov. J. Nucl. Phys. **6**, 552 (1968)].
[94]A. V. Ignatyuk and Yu. V. Sokolov, Yad. Fiz. **19**, 1229 (1974) [Sov. J. Nucl. Phys. **19**, 628 (1974)].
[95]D. L. Shpak, B. I. Fursov, and G. N. Smirenkin, Yad. Fiz. **12**, 35 (1970) [Sov. J. Nucl. Phys. **12**, 19 (1971)].
[96]L. G. Moretto *et al.*, Phys. Rev. **178**, 1845 (1969).
[97]V. Emma, S. Lo Nigro, and C. Milone, Nucl. Phys. **A199**, 186 (1973).
[98]G. L. Bate *et al.*, Phys. Rev. **131**, 722 (1963).
[99]R. F. Reising *et al.*, Phys. Rev. **141**, 1161 (1966).
[100]Yu. A. Nemilov *et al.*, Yad. Fiz. **2**, 460 (1965) [Sov. J. Nucl. Phys. **2**, 330 (1966)].

Translated by Julian B. Barbour